Cobalt-Dimer Nitrides: A Potential Novel Family of High-Temperature Superconductors

Yuhao Gu(顾雨豪)[1], Kun Jiang(蒋坤)[1,2], Xianxin Wu(吴贤新)[3], and Jiangping Hu(胡江平)[1,4*]

[1]*Beijing National Laboratory for Condensed Matter Physics, and Institute of Physics, Chinese Academy of Sciences, Beijing 100190, China*
[2]*School of Physical Sciences, University of Chinese Academy of Sciences, Beijing 100190, China*
[3]*Institute of Theoretical Physics, Chinese Academy of Sciences, Beijing 100190, China*
[4]*Kavli Institute of Theoretical Sciences, University of Chinese Academy of Sciences, Beijing 100190, China*

(Received 27 July 2022; accepted manuscript online 25 August 2022)

We predict that the square lattice layer formed by $[Co_2N_2]^{2-}$ diamond-like units can host high-temperature superconductivity. The layer appears in the stable ternary cobalt nitride, $BaCo_2N_2$. The electronic physics of the material stems from Co_2N_2 layers where the dimerized Co pairs form a square lattice. The low energy physics near Fermi energy can be described by an effective two-orbital model. Without considering interlayer couplings, the two orbitals are effectively decoupled. This electronic structure satisfies the "gene" character proposed for unconventional high-temperature superconductors. We predict that the leading superconducting pairing instability is driven from an extended s-wave ($s^{\pm}$) to a d-wave by hole doping, e.g., in $Ba_{1-x}K_xCo_2N_2$. This study provides a new platform to establish the superconducting mechanism of unconventional high-temperature superconductivity.

DOI: 10.1088/0256-307X/39/9/097401

Recently, we have proposed a roadmap to search for or to design unconventional high-temperature superconductors (T_c).[1,2] It is based on the idea that unconventional high T_c must host a certain electronic environment in which those d-orbitals of transition metal atoms with the strongest in-plane coupling to the p-orbitals of anions are isolated near Fermi energy. Both cuprates[3] and iron-based superconductors[4] host such an environment. This simple feature not only guarantees the superexchange antiferromagnetic interactions that are generated through d–p couplings can be maximized to provide superconducting pairing, but also explains why high T_c's are rare in nature. Thus, this electronic feature can be considered as the gene of unconventional high T_c's. Following this understanding, a few cases for cobalt or nickel compounds have been theoretically proposed.[1,5,6] Unfortunately, none of these cases has been realized experimentally because the "gene" condition is typically not favored energetically.

Isolating those d-orbitals to satisfy the gene condition always costs significant energy. Therefore, creating such an environment requires a specific lattice structure in which the energy cost can be compensated. For example, in cuprates, the energy cost of isolating the $d_{x^2-y^2}$ e_g orbital is compensated by lowering the $3t_{2g}$ in the perovskite-type of structure. In iron-based superconductors, the energy cost of isolating the t_{2g} orbitals in a tetrahedron environment is reduced by the hybridization of the e_g and some part of t_{2g} orbitals between two edge shared tetrahedrons. This hybridization is critical in creating the gene condition for a partially filled d-shell. The hybridization creates an empty hybridized band at high energy while leaving two near half-filled bands attributed to pure t_{2g} orbitals near Fermi energy in the d^6 configuration of Fe^{2+}. We have proposed that the gene condition can be created in a layer formed by corner-shared tetrahedrons,[5,7] in which all three t_{2g}'s can be isolated near Fermi energy for the d^7 configuration of Co^{2+}. However, forming such a layer is difficult because of too much energy cost in isolating all three anti-bonding t_{2g} orbitals.

In this Letter, we predict that a new gene exists for the d^7 configuration of Co^{2+} in layers formed by $[Co_2N_2]^{2-}$ diamond-like units as shown in Fig. 1(a). The layers appear in a ternary cobalt nitride, $BaCo_2N_2$ (BCN), which is structurally stable with minimum formation energy. Cobalt atoms are dimerized in a $[Co_2N_2]^{2-}$ unit. The dimers form a two-dimensional square lattice and their alignments alternate in two sublattices as shown in Fig. 1(b). We show that the electronic physics near Fermi energy can be described by an effective two-orbital model

*Corresponding author. Email: jphu@iphy.ac.cn

in the square lattice and satisfies the gene condition. There are strong antiferromagnetic interactions when electron-electron correlations are included. In particular, with hole doping, the Fermi surfaces can be driven from the iron-pnictide type with the simultaneous appearance of the hole and electron pockets [8–10] to the cuprate type with a single Fermi surface near half filling. [11] We predict that both extended s-wave ($s^{\pm}$) [9,10] and d-wave superconducting states can be formed in different doping regions. The transitional region between these two states may be featured by an s-wave and d-wave mixed superconducting state.

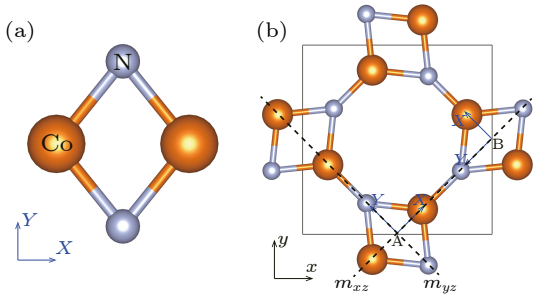

Fig. 1. (a) Structure of Co_2N_2 dimer. (b) Structure of Co_2N_2 layer. The dashed black lines show the mirror symmetries. X–Y coordinates are defined according to the direction of the Co–Co bond and x–y are the global coordinates in the conventional crystal structure.

Before presenting the detailed calculation, we use the symmetry analysis to argue why the electronic physics in the single Co_2N_2 layer is described by a two-orbital model and satisfies the gene condition. In a $[Co_2N_2]^{2-}$ unit in Fig. 1(a), the states from the d-orbitals form bonding ($d^{\rm B}$) and anti-bonding ($d^{\rm A}$) states. It is obvious that the bonding states, as well as the states from the d_{Z^2} orbital, have much lower energy and are irrelevant. We can focus on the four $d^{\rm A}$ states and classify them with respect to the XZ, YZ and XY mirror plane symmetries as shown in Fig. 2. The states can be labeled by the symmetry characters as $[d^{\rm A}_{XY}(-,-,+)$, $d^{\rm A}_{YZ}(-,-,-)$, $d^{\rm A}_{X^2-Y^2}(+,-,+)$, $d^{\rm A}_{XZ}(+,-,-)]$, where the signs represent the three mirror symmetries characters. In the first order approximation, we only need to consider the hoppings between the two nearest neighbor (NN) sites to determine the kinematics of these states. It is important to notice that the two dimers between two NN sites align perpendicularly. Therefore, only the electrons in those states with the same symmetry characters with respect to the XZ and YZ planes are allowed to hop between the two NN sites, namely, only the electrons in $d^{\rm A}_{XY}(-,-,+)$ and $d^{\rm A}_{YZ}(-,-,-)$ can generate NN hoppings, as illustrated in Fig. 2. The intra-orbital NN hopping within the other two states is forbidden due to the perpendicular alignment of the two NN dimers. We also notice that the d_{XY} and d_{YZ} orbitals are those orbitals with stronger d–p couplings. For the d^7 configuration of Co^{2+}, there are roughly two electrons left to fill the two bands. This rough analysis suggests that the electronic band structure of the Co_2N_2 layer can be described by a model with two decoupled orbitals and can satisfy the gene condition.

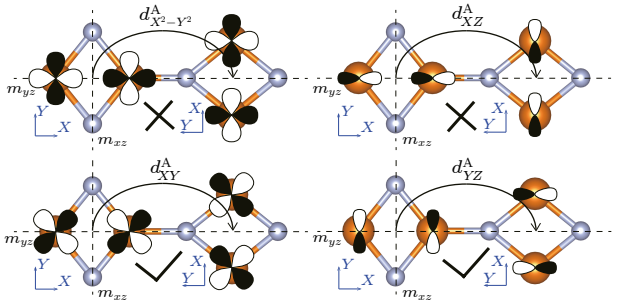

Fig. 2. Sketch of intra-orbital NN hopping between anti-bonding molecular orbitals of Co_2N_2 dimers. The intra-anti-bonding-orbital hoppings between the $d^{\rm A}_{X^2-Y^2}/d^{\rm A}_{XZ}$ molecular orbitals of two NN dimers are forbidden due to the opposite mirror symmetry eigenvalues while those between the $d^{\rm A}_{XY}/d^{\rm A}_{YZ}$ molecular orbitals are allowed.

To obtain the effective model in the monolayer Co_2N_2, we first analyze its symmetry. The point group at A/B site is D_{2h} and the anti-bonding states of Co d_{YZ} and d_{XY} belong to A_u and B_{1g} irreducible representations, respectively. They are decoupled in the monolayer due to the mirror reflection with respect to XY plane. Remarkably, there is a glide mirror operation $\{M_{xz/yz}|\frac{1}{2},\frac{1}{2}\}$, connecting the Co sites around A and B. This nonsymmorphic symmetry can be used to unfold the band structure into a one-sublattice lattice, analogous to iron-based superconductors (see our supporting information and its references [12–19] for more details). The effective Hamiltonian can be simplified to a two-orbital model on a square lattice. Based on the anti-bonding Co d_{XY} and d_{YZ} orbitals, the two-orbital tight-binding (TB) Hamiltonian reads

$$H_t = \sum_{\boldsymbol{k}\alpha\beta\sigma} \varepsilon^{\alpha\beta}_{\boldsymbol{k}} d^{\dagger}_{\boldsymbol{k}\alpha\sigma} d_{\boldsymbol{k}\beta\sigma} + \sum_{\boldsymbol{k}\sigma} e_{\alpha} d^{\dagger}_{\boldsymbol{k}\alpha\sigma} d_{\boldsymbol{k}\alpha\sigma}, \qquad (1)$$

where the operator $d^{\dagger}_{\boldsymbol{k}\alpha\sigma}$ ($d_{\boldsymbol{k}\alpha\sigma}$) creates (annihilates) an electron with momentum $\boldsymbol{k}$ of orbital α and spin σ, and e_{α} is the onsite energy for the α orbital. The hopping terms in Eq. (1) are given by

$$\varepsilon^{\alpha\beta}_{k} = [2t_{\alpha}(\cos k_X + \cos k_Y) + 4t'_{\alpha} \cos k_X \cos k_Y]\delta_{\alpha\beta}.$$

We fit our model to the DFT band structure of the monolayer Co_2N_2, and the fitting parameters are provided in Table 1. The corresponding TB band structure is shown in Fig. 3(d), in comparison to the DFT band structure. A reasonable agreement between them is reached.

Table 1. Hopping parameters of the TB model in eV.

Hopping integral	First (t_α)	Second (t'_α)	e_α
Intra-orbital t_{XY}	−0.30	−0.16	2.0
Intra-orbital t_{YZ}	−0.30	−0.02	0.2

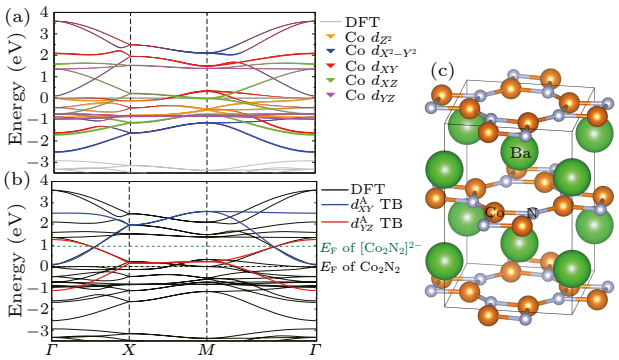

Fig. 3. (a) DFT-calculated band structure of Co_2N_2 monolayer and projected weight of d-orbital-like WFs in its symmetric local coordinate (X–Y coordinate). The coordinates in the abscissa are corresponding to the high symmetric $\boldsymbol{k}$-points of the tetragonal conventional cell's Brillouin zone. (b) Band structures of Co_2N_2 monolayer from DFT and our effective TB model. The black dotted line represents the Fermi level (E_F) of Co_2N_2 monolayer while the green dotted line represents the Fermi level (E_F) of $[Co_2N_2]^{2-}$. (c) Crystal structure of $BaCo_2N_2$ in the conventional cell.

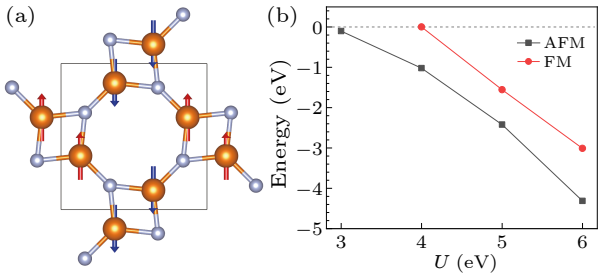

Fig. 4. (a) The in-plane AFM order of Co_2N_2 layer. (b) DFT+U-calculated energies of different magnetic orders of $BaCo_2N_2$ relative to the paramagnetic state as a function of the onsite U.

As unconventional superconductivity is usually in the vicinity of magnetic orders, we further study magnetic interactions in BCN by performing calculations including an onsite interaction U in Co sites (DFT+U).[19] We find that there are strong antiferromagnetic (AFM) interactions between two NN dimers in the tetragonal lattice in the presence of electron-electron correlations. In Fig. 4(a), we show the AFM configuration of the states, and in Fig. 4(b), we plot the energy gain of the state as a function of U relative to the paramagnetic state. When $U \geq 3\,\text{eV}$, the AFM state starts to have energy gain and becomes the ground state. By mapping the energies of different magnetic configurations into the Heisenberg model, we can estimate that the AFM interaction J between two NN dimers is about 16.0/13.5/20.4 meV when $U = 4/5/6\,\text{eV}$. This J between NN dimers is similar to J_2 between second-nearest neighboring (SNN) Fe atoms in iron-based superconductors.[20,21] This AFM interaction is clearly mediated by N atoms and arises from the superexchange mechanism.

Then, we can apply a strong correlation method to uncover the superconducting property of Co_2N_2 material. The correlation part of the Hamiltonian H_I follows the two-orbital Hubbard model:[22–25]

$$H_\text{I} = U\sum_{i,\alpha}\hat{n}_{i\alpha\uparrow}\hat{n}_{i\alpha\downarrow} + \Big(U' - \frac{1}{2}J_\text{H}\Big)\sum_{i,\alpha<\beta}\hat{n}_{i\alpha}\hat{n}_{i\beta} - J_\text{H}\sum_{i,\alpha\neq\beta}\boldsymbol{S}_{i\alpha}\cdot\boldsymbol{S}_{i\beta} + J_\text{H}\sum_{i,\alpha\neq\beta}d^\dagger_{i\alpha\uparrow}d^\dagger_{i\alpha\downarrow}d_{i\beta\downarrow}d_{i\beta\uparrow}, \tag{2}$$

where the intra and interorbital repulsion U and U' are related by Hund's rule coupling J_H through $U = U' + 2J_\text{H}$. The correlation parameters are set as $U = 2\,\text{eV}$ and $J_\text{H} = 0.1U$.

The strong correlation effects are studied using the multiorbital Gutzwiller projection method:[26–28] $H = H_\text{t} + H_\text{I} \rightarrow H_\text{G} = P_\text{G}H_\text{t}P_\text{G}$, where P_G is the finite-U Gutzwiller projection operator that reduces the statistical weight of the Fock states with multiple occupations. The projection can be conveniently implemented using the Gutzwiller approximation (GW),[26,27] which has been used in the multiorbital cobaltates,[29] Fe-pnictides,[28] and the monolayer CuO_2 grown on $Bi_2Sr_2CaCu_2O_{8+\delta}$ substrate.[30] In this approach, the Gutzwiller projected Hamiltonian is expressed as

$$H_\text{G} = \sum_{\boldsymbol{k}\alpha\beta\sigma} g^\sigma_{\alpha\beta}\varepsilon^{\alpha\beta}_{\boldsymbol{k}}d^\dagger_{\boldsymbol{k}\alpha\sigma}d_{\boldsymbol{k}\beta\sigma} + \sum_{\boldsymbol{k}\sigma}(e_\alpha + \lambda^\sigma_\alpha)d^\dagger_{\boldsymbol{k}\alpha\sigma}d_{\boldsymbol{k}\alpha\sigma}. \tag{3}$$

The strong correlation effects are described by the orbital dependent hopping renormalization $g^\sigma_{\alpha\beta}$ and the renormalized crystal field λ^σ_α, which must be determined self-consistently for a given electron density n.

The superexchange interactions involving spin-orbital can also be derived and the Kugel–Khomskii type terms are written as

$$H_\text{J-K} = \sum_{\langle ij\rangle}\Big[J\boldsymbol{S}_i\cdot\boldsymbol{S}_j + \sum_{\mu\nu}I_{\mu\nu}T^\mu_iT^\nu_j + \sum_{\mu\nu}K_{\mu\nu}(\boldsymbol{S}_i\cdot\boldsymbol{S}_j)(T^\mu_iT^\nu_j)\Big], \tag{4}$$

where the J-term is the $SU(2)$ invariant Heisenberg spin exchange coupling, while the terms proportional

$I_{\mu\nu}$ and $K_{\mu\nu}$ describe the anisotropic orbital and spin-orbital entangled superexchange interactions, respectively, since the orbital rotation symmetry is broken by the lattice in the hopping Hamiltonian $H_{\rm t}$. Decoupling the superexchange interactions by including all spin-singlet pairing order parameters,

$$\Delta_{ij}^{\alpha\beta\dagger} = d_{i\alpha\uparrow}^{\dagger} d_{j\beta\downarrow}^{\dagger} - d_{i\alpha\downarrow}^{\dagger} d_{j\beta\uparrow}^{\dagger}, \tag{5}$$

we can arrive at the effective Hamiltonian as

$$H = P_{\rm G} H_{\rm t} P_{\rm G} - \sum_{\langle ij\rangle} \Big[\frac{J_s}{2} \sum_{\alpha\beta} \Delta_{ij}^{\alpha\beta\dagger} \Delta_{ij}^{\alpha\beta} + \frac{K}{2} \sum_{\alpha\neq\beta} (\Delta_{ij}^{\alpha\alpha\dagger} \Delta_{ij}^{\beta\beta} + \Delta_{ij}^{\alpha\beta\dagger} \Delta_{ij}^{\beta\alpha}) \Big]. \tag{6}$$

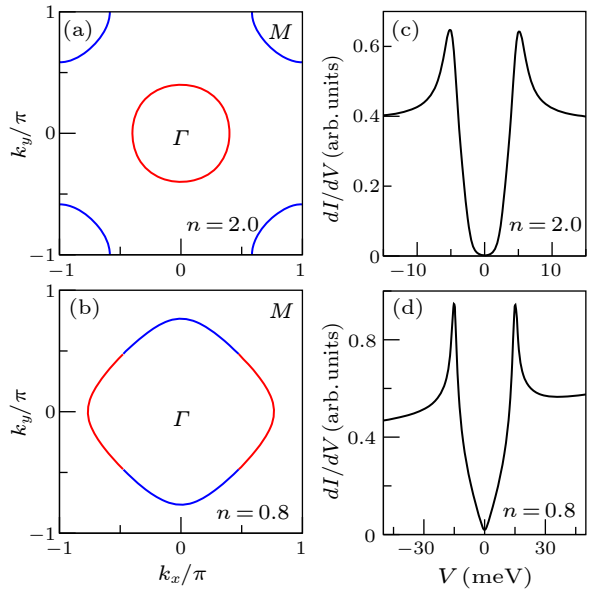

Fig. 5. (a) Fermi surface of Co_2N_2 at $n = 2.0$. An $s^{\pm}$-wave SC is obtained here. The Fermi pocket with red color corresponds to the $\Delta(k) > 0$ while the Fermi pocket with blue color corresponds to the $\Delta(k) < 0$ patch. (b) Fermi surface of Co_2N_2 at $n = 0.8$. A d-wave SC is obtained here. The FS with red color corresponds to the $\Delta(k) > 0$ patch while the FS with blue color corresponds to the $\Delta(k) < 0$ patch. (c) Local tunneling density of states at $n = 2.0$ with gap $\Delta = 5.2$ meV. A thermal broadening of 0.5 meV is used. (d) Local tunneling density of states at $n = 0.8$ with gap $\Delta = 15.2$ meV.

Using the GW approximation, we found two different regimes separating by a Lifshitz transition when hole doping the Co_2N_2. This Lifshitz transition point $n_{\rm L}$ is shifted from 0.86 at $U = 0$ to 1.12 at $U = 2$ eV owing to the correlation-induced crystal field renormalization. When electron density n is greater than $n_{\rm L}$, there are one hole pocket centering around the Γ point and one electron pocket centering around the M point respectively, as shown in Fig. 5(a) at $n = 2.0$. On the other hand, when n is less than $n_{\rm L}$, a Fermi surface (FS) centering around the Γ point is arrived, as shown in Fig. 5(b) at $n = 0.8$. In both the cases, Fermi surfaces are plotted in the unfolded Brillouin zone using the two-orbital model. These two regimes have different superconducting ground states.

In the low doping region, the physical property of Co_2N_2 is similar to the iron-based SC with two electron pockets. In iron-based SC, a nodaless $s^{\pm}$ wave SC is obtained from both strong coupling and weak coupling studies.[9,10] By choosing $J_s = 200$ meV and $K = 80$ meV, an $s^{\pm}$ wave with extend s-wave factor $\cos(k_x) + \cos(k_y)$ is also achieved from the above self-consistent mean field study. As shown in Fig. 5(a), the pairing gap $\Delta(k)$ at Fermi pocket around Γ is positive labeled with red color while $\Delta(k)$ at Fermi pocket around M is negative with blue color. To compare with scanning tunneling microscope, we also calculate the tunneling density of states (DOS). As shown in Fig. 5(c), a U-shape DOS spectrum is obtained with a coherent peak at $\Delta = 5.2$ meV, which further confirms the nodaless nature of this regime.

In the above region, both bands are still away from the half-filling of each band. Hence, the superconducting gap is relatively weak. After the Lifshitz transition $n_{\rm L}$, the lower band begins to close to its half-filling. Since the upper band is empty, the two-orbital model is down-folded to the single orbital model. In this regime ($n < n_{\rm L}$), a physical property similar to the cuprates SC is achieved. We choose the filling at $n = 0.8$, which is close to the optimal doping of cuprates. In this case, a d-wave superconductor with form factor $\cos(k_x) - \cos(k_y)$ is obtained as shown in Fig. 5(b). The $\Delta(k)$ around the FS breaks into four different patches, where the red patches show a positive gap and the blue patches show a negative gap. Furthermore, a V-shape tunneling DOS is calculated in Fig. 5(d), which is a hallmark for d-wave SC. A much larger SC gap with $\Delta = 15.2$ meV is obtained. Hence, a high-temperature SC with d-wave pairing can be achieved in the large hole doping Co_2N_2 material. In the transitional region, an s-wave and d-wave mixed superconducting state may also emerge owing to the high-order coupling between s-wave and d-wave in the free energy.[31–33]

In summary, we have proposed a new family of high-temperature superconductors consisting of $[Co_2N_2]^{2-}$ diamond-like units. These $[Co_2N_2]^{2-}$ units form a square lattice layer. The low energy physics near Fermi energy of the layer is described by an effective decoupled two-orbital model. This electronic structure satisfies the gene character proposed for unconventional high-temperature superconductors as both orbitals isolated near Fermi energy generate large dispersions through d–p couplings.

The system can bridge the gap between the elec-

tronic physics of iron-based SC and cuprates. Without doping ($n = 2.0$), the Fermi surface topology of the system is very similar to those of iron-pnictides with one electron pocket at the Brillouin zone center and one hole pocket at the Brillouin zone corner. In this case, an extended s-wave ($s^{\pm}$) pairing similar to iron-based SC is found using a strong-coupling mean-field study. However, at large hole doping close to $n = 1.0$, d-wave superconductivity similar to cuprates is achieved. The transitional region between these two SC states will be an extremely interesting region to study both theoretically and experimentally in the future.

The layer is stabilized in $BaCo_2N_2$. $BaCo_2N_2$ is the stablest Ba–Co–N ternary structure in its stoichiometric ratio according to the Materials Project database.[34] The hole doping can be achieved by substituting Ba with K as $Ba_{1-x}K_xCo_2N_2$. Thus, successfully synthesizing $BaCo_2N_2$ or related materials can establish a platform to decode the superconducting mechanism of unconventional high-temperature superconductivity.

Acknowledgment. This work was supported by the National Key Basic Research Program of China (Grant No. 2017YFA0303100), the National Natural Science Foundation of China (Grant Nos. 11888101 and 12174428), the Strategic Priority Research Program of Chinese Academy of Sciences (Grant No. XDB28000000), and the Chinese Academy of Sciences Project for Young Scientists in Basic Research (Grant No. YBR-048).

References

[1] Hu J, Le C, and Wu X 2015 *Phys. Rev. X* **5** 041012
[2] Hu J 2016 *Sci. Bull.* **61** 561
[3] Bednorz J G and Müller K A 1986 *Z. Phys. B* **64** 189
[4] Kamihara Y, Watanabe T, Hirano M, and Hosono H 2008 *J. Am. Chem. Soc.* **130** 3296
[5] Hu J and Le C 2017 *Sci. Bull.* **62** 212
[6] Le C, Qin S, and Hu J 2017 *Sci. Bull.* **62** 563
[7] Hu J, Gu Y, and Le C 2018 *Sci. Bull.* **63** 1338
[8] Poltavets V V, Greenblatt M, Fecher G H, and Felser C 2009 *Phys. Rev. Lett.* **102** 046405
[9] Seo K J, Bernevig B A, and Hu J P 2008 *Phys. Rev. Lett.* **101** 206404
[10] Hirschfeld P J, Korshunov M M, and Mazin I I 2011 *Rep. Prog. Phys.* **74** 124508
[11] Damascelli A, Hussain Z, and Shen Z X 2003 *Rev. Mod. Phys.* **75** 473
[12] Kresse G and Furthmüller J 1996 *Phys. Rev. B* **54** 11169
[13] Kresse G and Joubert D 1999 *Phys. Rev. B* **59** 1758
[14] Perdew J P, Burke K, and Ernzerhof M 1996 *Phys. Rev. Lett.* **77** 3865
[15] Mostofi A A, Yates J R, Lee Y S, Souza I, Vanderbilt D, and Marzari N 2008 *Comput. Phys. Commun.* **178** 685
[16] Marzari N, Mostofi A A, Yates J R, Souza I, and Vanderbilt D 2012 *Rev. Mod. Phys.* **84** 1419
[17] Jiang K, Hu J, Ding H, and Wang Z 2016 *Phys. Rev. B* **93** 115138
[18] Gu Y, Wu X, Jiang K, and Hu J 2021 *Chin. Phys. Lett.* **38** 017501
[19] Liechtenstein A, Anisimov V I, and Zaanen J 1995 *Phys. Rev. B* **52** R5467
[20] Ma F, Ji W, Hu J, Lu Z Y, and Xiang T 2009 *Phys. Rev. Lett.* **102** 177003
[21] Zeng J, Qing S, Le C, and Hu J 2017 *Phys. Rev. B* **96** 174506
[22] Castellani C, Natoli C R, and Ranninger J 1978 *Phys. Rev. B* **18** 4945
[23] Georges A, de Medici L, and Mravlje J 2013 *Annu. Rev. Condens. Matter Phys.* **4** 137
[24] Kugel K I and Khomskii D I 1973 *Sov. Phys.-JETP* **37** 725
[25] Kugel K I and Khomskii D I 1982 *Sov. Phys. Usp.* **25** 231
[26] Bunemann J, Weber W, and Gebhard F 1998 *Phys. Rev. B* **57** 6896
[27] Lechermann F, Georges A, Kotliar G, and Parcollet O 2007 *Phys. Rev. B* **76** 155102
[28] Zhou S and Wang Z 2010 *Phys. Rev. Lett.* **105** 096401
[29] Zhou S, Gao M, Ding H, Lee P A, and Wang Z 2005 *Phys. Rev. Lett.* **94** 206401
[30] Jiang K, Wu X, Hu J, and Wang Z 2018 *Phys. Rev. Lett.* **121** 227002
[31] Ren Y, Xu J H, and Ting C S 1996 *Phys. Rev. B* **53** 2249
[32] Matsumoto M and Shiba H 1996 *J. Phys. Soc. Jpn.* **65** 2194
[33] Li Q P, Koltenbah B E C, and Joynt R 1993 *Phys. Rev. B* **48** 437
[34] Jain A, Ong S P, Hautier G, Chen W, Richards W D, Dacek S, Cholia S, Gunter D, Skinner D, Ceder G, and Persson K A 2013 *APL Mater.* **1** 011002

Supporting Information for Cobalt-Dimer Nitrides: A Potential Novel Family of High Temperature Superconductors

Yuhao Gu,[1] Kun Jiang,[1,2] Xianxian Wu,[3] and Jiangping Hu[1,4,*]

[1]*Beijing National Laboratory for Condensed Matter Physics, and Institute of Physics, Chinese Academy of Sciences, Beijing 100190, China*
[2]*School of Physical Sciences, University of Chinese Academy of Sciences, Beijing 100190, China*
[3] *Institute of Theoretical Physics, Chinese Academy of Sciences, Beijing 100190, China*
[4]*Kavli Institute of Theoretical Sciences, University of Chinese Academy of Sciences, Beijing 100190, China*

(Dated: August 31, 2022)

COMPUTATIONAL METHODS

We employ the Vienna *ab initio* simulation package (VASP) code[1] with the projector augmented wave (PAW) method[2] to perform DFT calculations. The Perdew-Burke-Ernzerhof (PBE)[3] exchange-correlation functional is used in our calculations. The kinetic energy cutoff is set to be 600 eV for expanding the wave functions into a plane-wave basis in VASP calculations. We use the primitive cell of $BaCo_2N_2$ to calculate its electronic structure. The crystal structure is fully relaxed while the force convergence criterion is 0.005 eV/Å. The energy convergence criterion is 10^{-7} eV and the Γ-centered **k**-mesh is $12 \times 12 \times 12$. The Co_2N_2 monolayer is extracted from the relaxed bulk $BaCo_2N_2$ with 40Å thick vacuum layer and its Γ-centered **k**-mesh is $16 \times 16 \times 1$.

We employ Wannier90[4, 5] to calculate maximally localized Wannier functions in $BaCo_2N_2$, which perfectly reproduces DFT-calculated band structure around the Fermi level. The initial projectors are Co's d-orbitals with local symmetric $X - Y$ coordinate.

In the study of the magnetism of $BaCo_2N_2$, the DFT+U method in the formulation of Liechtenstein et al. [8] is employed to describe the associated electron-electron correlation effect and J is fixed as $\frac{U}{4}$. To estimate the magnetic exchange between two NN dimers, the energies of different magnetic states are calculated with the relaxed structure of paramagnetic $BaCo_2N_2$.

EXPLICIT FORM OF 4-BAND TB MODEL

The 4-band effective tight-binding (TB) model before unfolding with the basis of the d_{XY} and d_{YZ} orbitals is given by

$$H_t^{4-band} = \sum_{k\alpha\beta ij} \varepsilon_k^{\alpha\beta ij} d_{k\alpha i}^\dagger d_{k\beta j} + \sum_{ki} e_\alpha d_{k\alpha i}^\dagger d_{k\alpha i}, \tag{1}$$

where α/β is the orbital index, i/j is the site index and e_α denotes the crystal field energy of each orbital. The corresponding expressions for the hopping energies in Eq. (1) are given by

$$\varepsilon_k^{\alpha\alpha AA} = \varepsilon_k^{\alpha\alpha BB} = 2t'_\alpha(\cos k_x + \cos k_y); \tag{2}$$

$$\varepsilon_k^{\alpha\alpha AB} = \varepsilon_k^{\alpha\alpha BA} = 4t_\alpha \cos\frac{k_x}{2}\cos\frac{k_y}{2}. \tag{3}$$

As mentioned in our main text, we can transfer the 4×4 TB model into a block-diagonalized matrix with using the glide symmetry:

$$H^{eff}(\boldsymbol{k}) = U H_t^{4-band} U^\dagger = \begin{pmatrix} H_t(\boldsymbol{k}) & 0 \\ 0 & H_t(\boldsymbol{k+Q}) \end{pmatrix}, \tag{4}$$

here H_k is the effective two-band model in our main text and $Q = (\pi, \pi)$ is the folding vector. The unitary transformation U is defined as

$$U = \frac{1}{\sqrt{2}} \begin{pmatrix} 1 & 0 & 1 & 0 \\ 0 & 1 & 0 & 1 \\ 1 & 0 & -1 & 0 \\ 0 & 1 & 0 & -1 \end{pmatrix}, \tag{5}$$

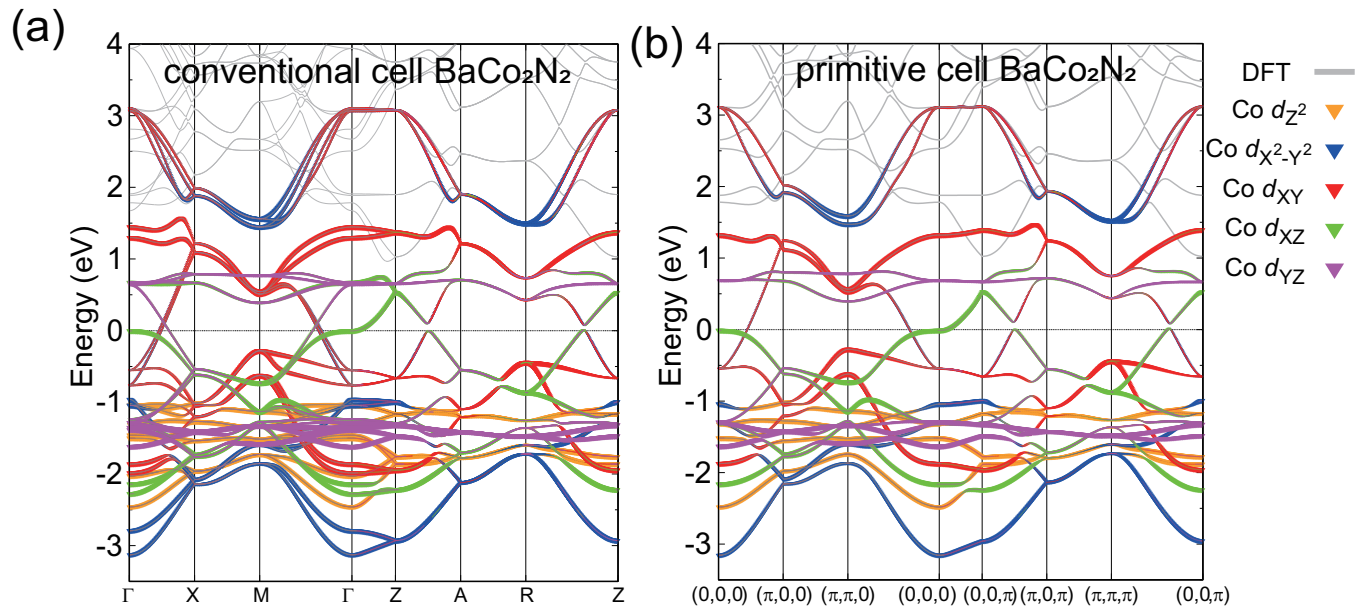

FIG. S1: DFT-calculated band structures of $BaCo_2N_2$ and projected weight of d-orbital-like WFs in its symmetric local coordinate (X-Y coordinate) with (a) the conventional cell and (b) the primitive cell. The coordinates in the abscissa of (b) are corresponding to the high symmetric **k**-points of the tetragonal conventional cell's Brillouin zone.

which is similar to that in FeSe[6] and $BaCuS_2$[7].

BAND STRUCTURE OF $BaCo_2N_2$

Fig.S1 shows the orbital-resolved band structure from DFT calculations of $BaCo_2N_2$. The N p orbitals, absent in the figure, are located around 3.5 eV below the Fermi level, while Co 3d orbitals dominate from -3 eV to 3 eV. Despite moderate inter-orbital coupling, low-energy bonding states and high-energy anti-bonding states for each Co 3d orbital can be identified. We also notice that the dispersion of band structure around the Fermi level is similar with that in Co_2N_2 monolayer, which is consistent with our previous qualitative analysis from symmetry.

* Electronic address: jphu@iphy.ac.cn

[1] G. Kresse and J. Furthmüller, Phys. Rev. B 54, 11169 (1996).
[2] G. Kresse and D. Joubert, Phys. Rev. B 59, 1758 (1999).
[3] J. P. Perdew, K. Burke and M. Ernzerhof, Phys. Rev. Lett. 77, 3865 (1996).
[4] A. A. Mostofi, J. R. Yates, Y.-S. Lee, I. Souza, D. Vanderbilt, and N. Marzari, Comput. Phys. Commun. 178, 685 (2008).
[5] N. Marzari, A. A. Mostofi, J. R. Yates, I. Souza, and D. Vanderbilt, Rev. Mod. Phys. 84,1419 (2012).
[6] K. Jiang, J. Hu, H. Ding, and Z. Wang, Phys. Rev. B **93**, 115138 (2016).
[7] Y. Gu, X. Wu, K. Jiang, and J. Hu, Chin. Phys. Lett. **38**, 017501 (2021).
[8] A. Liechtenstein, V. I. Anisimov, and J. Zaanen, Phys. Rev. B 52, R5467 (1995).